

International Journal of Advance Research in Computer Science and Management Studies

Research Article / Survey Paper / Case Study

Available online at: www.ijarcsms.com

An Efficient Multimodal Medical Volumetric Data Fusion Using 3d Wavelet Transform and Fusion Rule

S.Sadhana¹

Pg Scholar,
Department Of Medical Electronics,
Avinashilingam University, Coimbatore,
Tamilnadu, India.

J.Revathi²

Asst. Professor,
Faculty Of Engineering,
Avinashilingam University, Coimbatore,
Tamilnadu, India

Abstract: The main objective of image fusion is to obtain useful complementary information from multimodality images into final image as much as possible. A number of algorithms for image fusion have been proposed till date. The main aim in image fusion of medical images is to preserve the edge information and contrast because recent image fusion algorithm is prone to reduce the contrast of the fused image. One of the simplest methods to obtain the salient features of both the images into a fused image is just average. Most of the image fusion algorithm aims at obtaining as much as possible information in the fused image, with keeping the error low as possible between the fused image and input image. The resulting image will be more informative than any of the input images. In case of medical images, contains more contrast and edge-like information, which needs to be preserved in fused image. In this paper I have proposed and compared methods to preserve contrast and edge information as much as possible using wavelet transform. The image fusion techniques allow the integration of different information sources. The fused image can have complementary spatial and spectral resolution characteristics

Keywords: image fusion; luminance extraction; image separation; wavelet transform.

I. INTRODUCTION

NEED FOR THE STUDY: Multimodal medical image fusion technologies facilitate better applications of medical imaging for they provide an easy access for doctors to recognize the lesion structures and functional change by studying the data of anatomical and functional modalities. The fusion of medical images has proved to be useful for advancing the clinical reliability of using medical imaging for medical diagnostics and analysis, and is a scientific discipline that has the potential to significantly grow in the coming years. For example, the combination of the Positron Emission Tomography (PET) and Computed Tomography (CT) imaging can be used to concurrently view the tumor activity by visualizing the anatomical and physiological characteristics in oncology. The fusion of CT and Magnetic Resonance Imaging (MRI) is helpful for the Neuro-navigation in skull base tumor surgery and the combination of the PET and MRI is useful for the diagnosis of the hepatic metastasis. Due to the great need in practical applications, different fusion technologies have been developed in recent years, all of which can be generally classified into three levels: pixel level, feature level, and decision level. Medical Image Fusion usually employs the techniques at the pixel level. According to whether the multi - scale decomposition (MSD) is applied, the pixel level fusion methods can be roughly classified into MSD-based or non-MSD-based methods. Compared to the latter, the former performs better for salient image features that can be captured in different scales, which are more suitable to the mechanism of the human vision.

But, the standard image fusion techniques can distort the spectral information of the multispectral data, while merging. The medical imaging has attracted increasing attention due to its critical role in health care. However, different types of imaging techniques such as X-ray, computed tomography (CT), magnetic resonance imaging (MRI), magnetic resonance angiography

(MRA), etc., provide limited information where some information is common, and some are unique. For example, X-ray and computed tomography (CT) can provide dense structures like bones and implants with less distortion, but it cannot detect physiological changes. Similarly, normal and pathological soft tissue can be better visualized by MRI image, whereas PET can be used to provide better information on blood flow and flood activity with low spatial resolution. As a result, the anatomical and functional medical images are needed to be combined for a compendious view (Figure 1-3). For this purpose, the multimodal medical image fusion has been identified as a promising solution which aims to integrate information from multiple modality images to obtain a more complete and accurate description of the same object. Multimodal medical image fusion not only helps in diagnosing diseases, but it also reduces the storage cost by reducing storage to a single fused image instead of multiple-source images.

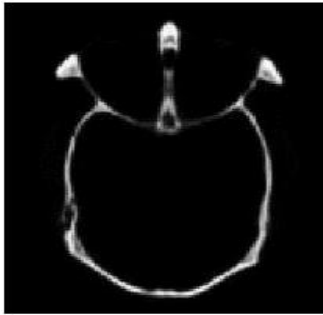


Fig.1.1 Input Image (CT)

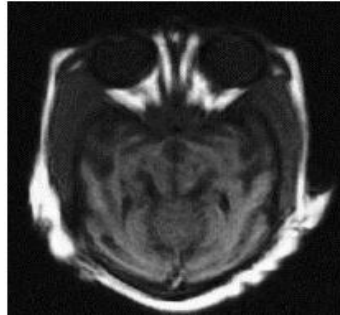


Fig.1.2 Input Image (MRI)

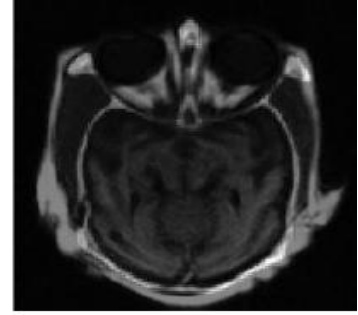


Fig.1.3 Output Image of (M-I)

II. REVIEW OF LITERATURE

J. Goutsias and H. J. A. M. Heijmans (2000) proposed a general axiomatic pyramid decomposition scheme for signal analysis and synthesis. This scheme comprises the following ingredients: (i) the pyramid consists of (finite or infinite) number of levels, such that the information, content decreases towards higher levels; (ii) each step towards a higher level is constituted by an (information-reducing) analysis operator, whereas each step towards a lower level is modeled by an (information-preserving) synthesis operator [1]. In 2003 G. Piella proposed an overview on image fusion techniques using multi-resolution decompositions. The aim is (i) to reframe the multi-resolution-based fusion methodology into a common formalism and within this framework, (ii) to develop a new region-based approach which combines aspects of both object and pixel-level fusion. The basic idea is to make a multi-resolution segmentation based on all different input images and to use this segmentation to guide the fusion process [2]. V. S. Petrovic and C. S. Xydeas (2004) have identified a novel approach to multi resolution signal-level image fusion for accurately transferring visual information from any number of input image signals, into a single fused image without loss of information or the introduction of distortion. The proposed system uses a "fuse-then-decompose" technique realized through a novel, fusion/decomposition system architecture [3].

G. Pajares and J. M. de la Cruz (2004) proposed the objective of image fusion to combine information from multiple images of the same scene. The result of image fusion is a new image which is more suitable for human and machine perception or further image-processing tasks such as segmentation, feature extraction and object recognition. Different fusion methods have been proposed in literature, including multi resolution analysis. This paper is an image fusion tutorial based on wavelet decomposition, i.e. a multi resolution image fusion approach. We can fuse images with the same or different resolution level, i.e. range sensing, visual CCD, infrared, thermal or medical. The tutorial performs a synthesis between the multi scale-decomposition-based image approaches [4]. G. Easley, et.al. (2008) In spite of their remarkable success in signal processing applications, it is now widely acknowledged that traditional wavelets are not very effective in dealing multidimensional signals containing distributed discontinuities such as edges. To overcome this limitation, one has to use basis elements with much higher directional sensitivity and of various shapes, to be able to capture the intrinsic geometrical features of multidimensional phenomena. This paper introduces a new discrete multi-scale directional representation called the discrete shearlet transform [5]. Q. Miao, et.al. (2011) have proposed in their paper that as shearlet transform has the features of directionality, localization,

anisotropy and multi scale, it is introduced into image fusion to obtain a fused image. The image could be decomposed by shearlet transform in any scale and any direction, and the detail information can be caught easily. Several different experiments are adopted to demonstrate that the fusion results based on shearlet transform contain more detail and smaller distortion information than any other methods does [6].

L. Wang, B. Li and L. F. Tian (2012) studied that the two-state Hidden Markov Tree (HMT) model can be extended into the SIST domain to describe the dependent relationships of the SIST coefficients of the cross-scale and inter-subbands. Based on the model, the paper explains why the conventional Average–Maximum fusion scheme is not the best rule for medical image fusion, and therefore a new scheme is developed, where the probability density function and standard deviation of the SIST coefficients are employed to calculate the fused coefficients. Finally, the fused image is obtained by directly applying the inverse SIST [7]. Y. Cao, Sh. Li, and J. Hu (2011) has proposed a method in which the source images are decomposed by non-subsampled shear let transform first and then the decomposition coefficients are merged according to the given fusion rule. Finally the fused image is reconstructed by inverse non-subsampled shear let transform. The experimental results over five pairs of registered multi-focus images and one pair of mis-registered multi-focus images demonstrate the superiority of the proposed method [8]. R. Shen et.al. (2013) have presented their work on Joint analysis of medical data collected from different imaging modalities which has become a common clinical practice. In this paper, they have proposed a novel cross-scale fusion rule for multi scale-decomposition-based fusion of volumetric medical images taking into account both intrascale and interscale consistencies [9].

III. METHODOLOGY

3.1 Proposed System Architecture

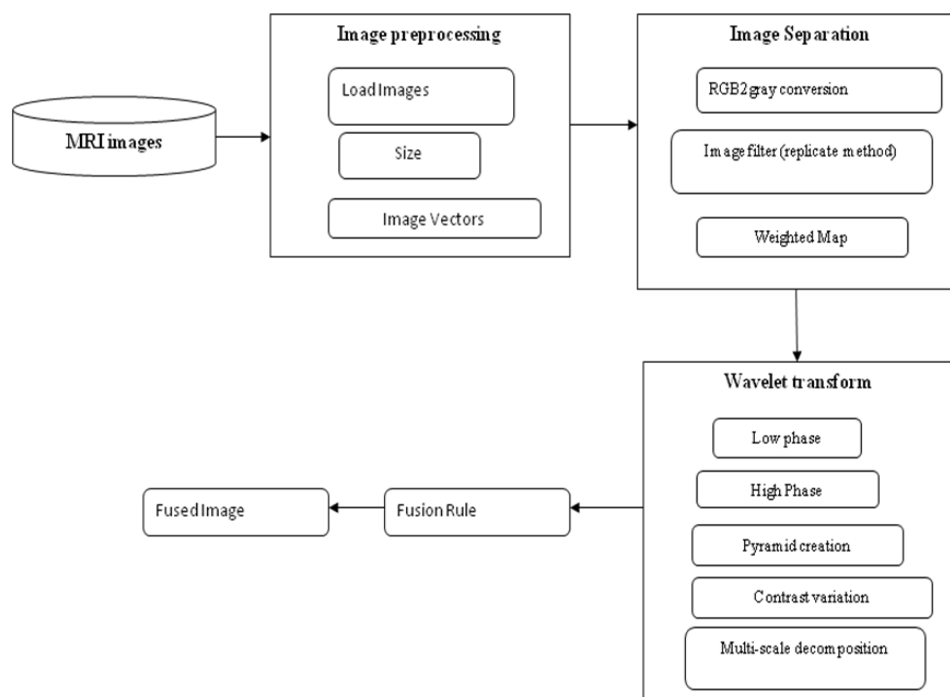


Fig. 3.1. Block Diagram of Proposed System Architecture

3.2 Algorithm for Image Separation

The MRI Image fusion of Depth of Field estimation algorithm design as follows,

- Step 1: The input four images are grouped into a single parameter with the help of vectorization concept.
- Step 2: To load the image sequence with corresponding scaling and each image is converted into double precision.
- Step 3: Double should be overloaded for all objects where it makes sense to convert it into a double precision value.

Step 4: In case of some of the images has different scaling then the difference in scaling is resized.

Step 5: To compute the DOF measures and combines them into a weight map.

Step 6: The RGB Input image vector is converted into Grayscale vector with help of rgb2gray Matlab in- built function.

Step 7: Using imfilter function: N-D filtering of multidimensional images.

Step 8: The output, is computed using double-precision floating point. If the image is an integer or logical array, then output elements that exceed the range of the given type are truncated, and fractional values are rounded.

4.2.6 Algorithm for Gradient Direction Estimation

Step 1: To compute the first order derivative of input Image vectors I in X , and in Y direction

Step 2: Assign the size of the image plot in the image vector space.

Step 3: To calculate the absolute value of X and Y co-ordinates.

Step 4: Assign the mesh grid function to be imaged plot.

Step 5: Process the gradient function along with the grid value of X and Y directions.

Step 6: To fill the directions with the help of quiver plot.

4.2.7 Algorithm or Luminance Extraction

Step 1: The input images acquired must be calibrated (dark frame and flat field) in the gradient direction estimation.

Step 2: The MRI image which was taken at a lower resolution must be resized (and re-sampled) to match the higher resolution of the luminance.

Step 3: To enhance the image vector using Gaussian and Laplacian filter.

Step 4: The next step begins the process of composting the Luminance of RGB.

Step 5: Next, make the luminance transparent by changing the opacity to approximately 70%.

4.2.8 Algorithm For MRI Image Fusion Process

Step 1: Resize the low resolution multispectral images to the same size as the panchromatic image.

Step 2: Transform the R, G and B bands of the multispectral image into Gray components.

Step 3: Modify the panchromatic image with respect to the multispectral image. This is usually performed by histogram matching of the panchromatic image with Intensity component of the multispectral images as reference.

Step 4: Replace the intensity component of the panchromatic image and perform the inverse transformation to obtain a high resolution multispectral image.

IV. RESULTS

In the proposed method suggested for fusion using wavelet transform, various measures such as DOF, Luminance and the contrast measure form the weighted map. The input images fed to the laplacian filter effectively fuses with the weighted map from the Gaussian filter. Speed has been improved in terms of time congruency and directive contrast. Global rule applied here captures the global information so that the loss of between slice information is out of question which is reported as a drawback. Fusion not only helps in perfect diagnosis, but also reduces storage to a single fused image instead of multiple sources.

The PSNR and SSIM values are calculated for the output fused image and the input multispectral image and are compared with the other methods and the graphical representation of the quality metrics are shown.

The brain structure information on the MRI are all well preserved together with the color information of the MRI images used for fusion. Therefore, the fusion results of the proposed method provided better visual sensing. Experimental results show that this algorithm effectively retains the detailed information of the original images and enhance their edge and texture features. The final fused image obtained through my fusion process well preserve the detailed texture features and colour information. Performance metrics given below show that this new algorithm is better than other methods compared.

4.1 Results

Fig.4.1 shows the input Images which are to be fused, the panchromatic and the multispectral image.

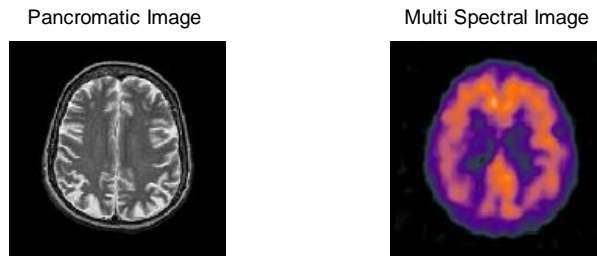


Fig. 4.1 Input Images

The depth of field estimation of the input images are calculated from the formula $d = \lambda / (n \sin^2(\alpha))$ as shown in Fig.4.2

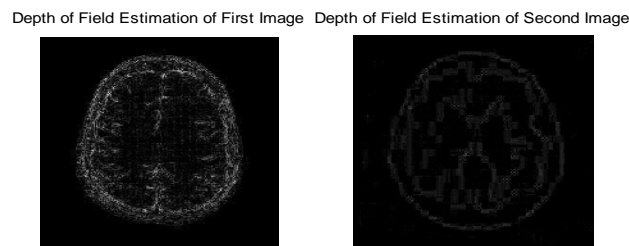


Fig. 4.2 Depth of Field Estimation

The orientation estimation or the gradient filter direction of images are obtained as shown in Fig 4.3. The red lines which are plotted using quiver plot shows the gradient measure. The pixel positions are estimated along with x and y coordinates.

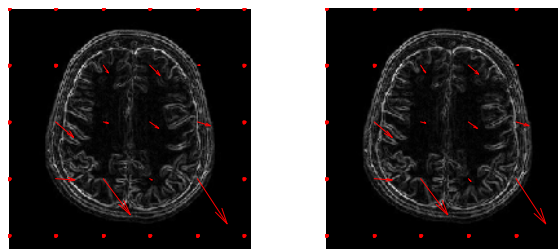


Fig.4.3 Gradient Filter Direction of Images

The image luminance is calculated for each point (x,y), which maximizes the visible contrast as shown in Fig 4.4.

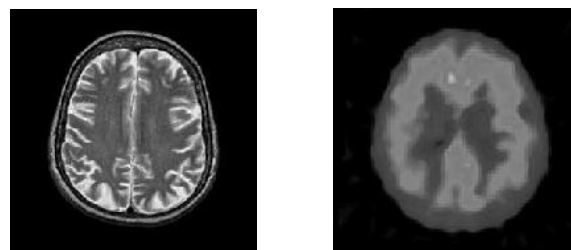


Fig. 4.4 Luminance Measure of Images

Stronger visible contrast for each point is adjusted to the incident light quantity and visibility of the contrast is enhanced and the contrast measure is shown as in Fig 4.5

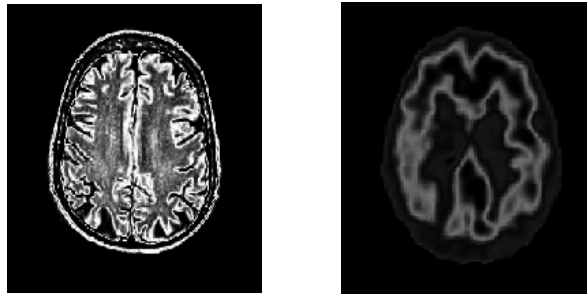


Fig. 4.5 Contrast Measure of Images

First level DWT for first image is performed which results in four components such as the Approximation Component(A1), Horizontal Component(H1), Vertical Detail(V1), Diagonal Detail(D1) as shown in Fig 4.6.

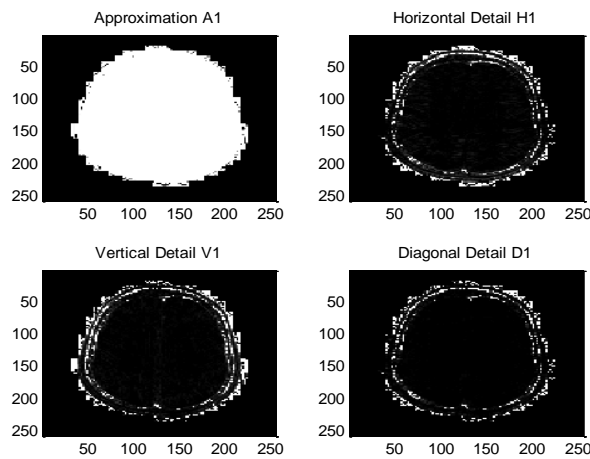


Fig. 4.6 First Level DWT of First Image

The Second level DWT of First image is performed and the results are obtained as shown in Fig 4.7

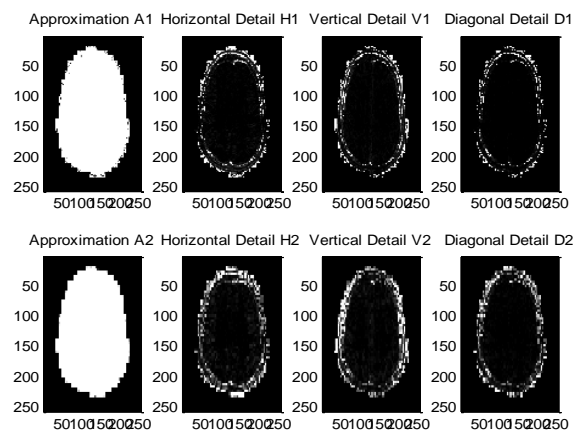


Fig. 4.7 Second Level DWT of First Image

The Analysis Reflect Edges Using Pyramid of First Image after second level of DWT are shown in Fig 4.8. Analysis synthesis are often implemented by hierarchical sub sampling leading to a pyramid and the analysis filter edge reflection of first image is shown in Fig 4.9.

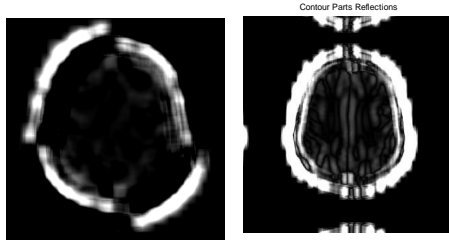


Fig 4.8 Analysis Reflect Edges Using Pyramid of First Image

Fig. 4.9 Analysis Filter Edge Reflection of First Image

First level DWT for Second image is performed which results in four components such as the Approximation Component(A1), Horizontal Component(H1), Vertical Detail(V1), Diagonal Detail(D1) as shown in Fig 4.10

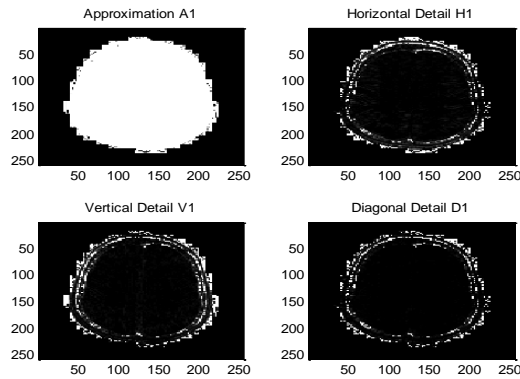


Fig. 4.10 First Level DWT of Second Image

The Second level DWT of second image is performed and the results are obtained as shown in Fig 4.11

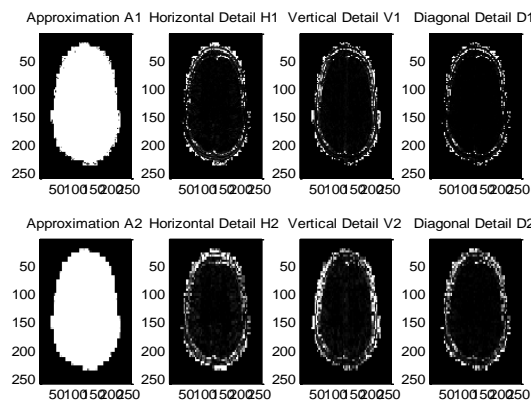


Fig. 4.11 Second Level DWT of Second Image

The Analysis Reflect Edges Using Pyramid of First Image after second level of DWT are shown in Fig 4.12. Analysis synthesis are often implemented by hierarchical sub sampling leading to a pyramid and the analysis filter edge reflection of second image is shown in Fig 4.13.

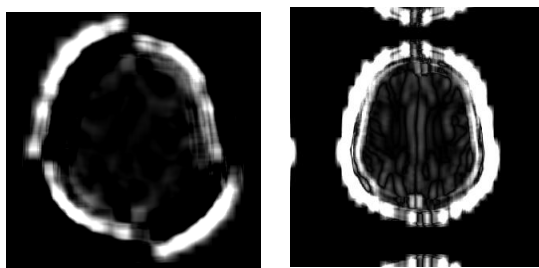


Fig. 4.12 Analysis Reflect Edges Using Pyramid of Second Image

Fig. 4.13 Analysis Filter Edge Reflection of Second Image

The weighted map calculated from depth of field, luminance and contrast are fed to the Gaussian filter and the input images to the Laplacian filter. The resulting image is decomposed into Laplacian pyramid which is the gray scale version of each image is shown in Fig 4.14.

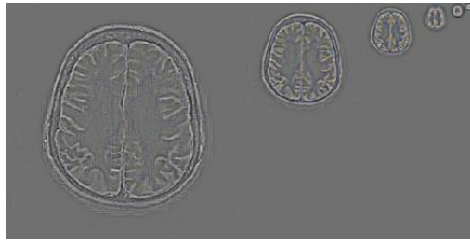


Fig. 4.14 Pyramid Formation and Fusion

Final fusion of the panchromatic and the multispectral image into a fused image is shown in Fig 4.15. That yields a simple color indicator (RGB) for contrast. The final fused image well preserves the edges and textures.

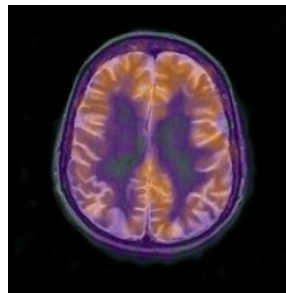


Fig. 4.15 Final Fusion Result

The PSNR value is calculated for the final fused image and the input spectral image and found to be high compared to the other methods as shown in Fig 4.16.

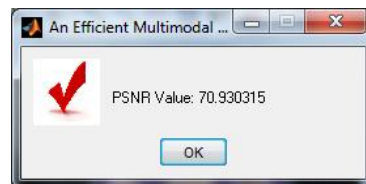


Fig. 4.16 PSNR Value

The SSIM value is calculated for the final fused image and the input spectral image and found to be high compared to the other methods as shown in Fig 4.17.

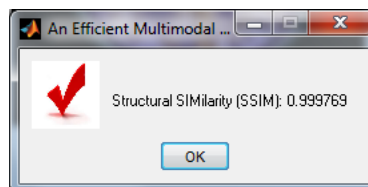


Fig. 4.17 SSIM Value

The total execution time for fusion process is shown in Fig 4.18.

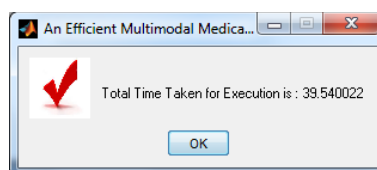


Fig. 4.18 Total Execution Time

4.2 Performance Metrics

The PSNR and SSIM values for various methods are tabulated and the graphical representation is also shown in Fig 4.19 which concludes that the proposed method is much better than the existing method.

Table 4.1 Average Value of the Evaluation Results for MRI Images with Noise

METHODS	LP	WAVELET	SHEARLET	SHEARLET GLOBAL-TO-LOCAL RULE	PROPOSED
PSNR	15.66	16.32	16.19	16.76	70.933
SSIM	0.51	0.61	0.62	0.65	0.99977

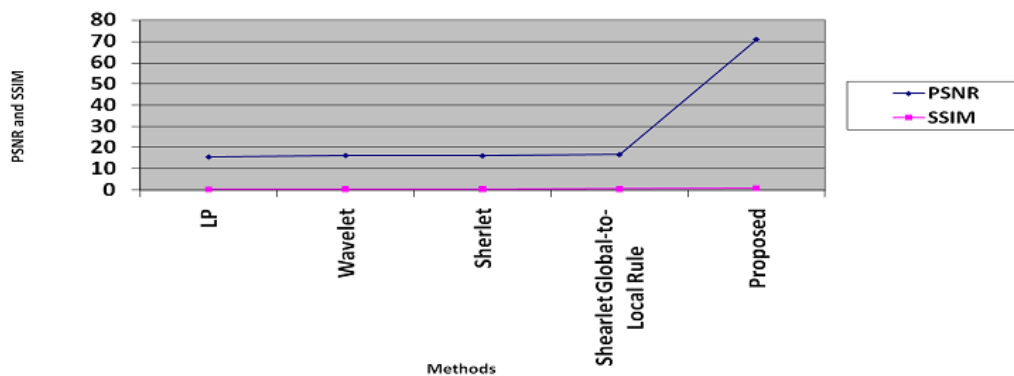


Fig 4.19 Graphical representation of Quality metrics

V. DISCUSSION AND CONCLUSION

5.1 DISCUSSION

An efficient Fusion Algorithm based on Wavelet Transform show that it effectively retain the detailed information of original images and enhance their texture features. Speed has been improved in terms of time congruency and directive contrast. Global rule applied here captures the global information so that the loss of between slice information is out of question which is reported as a drawback. Fusion not only helps in perfect diagnosis, but also reduces storage to a single fused image instead of multiple sources.

5.2 CONCLUSION

The fusion results of the proposed method yielded better PSNR and SSIM values from the performance metrics compared to the existing method and retains the detailed information of the original image and enhanced edge and texture features.

5.3 FUTURE SCOPE

The future scope of my proposed work is to put effort on normalization and to increase the resolution of the image.

References

1. A. L. Grosu, W. A. Weber, and M. Franz, "Reirradiation of recurrent highgrade gliomas using amino acid PET (SPECT)/CT/MRI image fusion to determine gross tumor volume for stereotactic fractionated radiotherapy," *Int. J. Rad. Oncol. Biol. Phys.*, vol. 73, pp. 511–519, 2005.
2. S. F. Nemeç, M. A. Donat, S. Mehraïn, K. Friedrich, C. Krestan, C. Matula, H. Imhof, and C. Czerny, "CT-MR image data fusion for computer assisted navigated neurosurgery of temporal bone tumors," *Eur. J. Radiol.*, vol. 62, pp. 192–198, 2007.
3. O. F. Donati, T. F. Hany, and C. S. Reiner, "Value of retrospective fusion of PET and MR images in detection of hepatic metastases: Comparison with 18F-FDG PET/CT a Gd-EOB-DTPA-enhanced MRI," *J. Nucl. Med.*, vol. 51, no. 5, pp. 692–699, 2010.
4. G. Piella, "A general framework for multi-resolution image fusion: From pixels to regions," *Inf. Fusion*, vol. 4, no. 4, pp. 259–280, 2003.

5. J.Goutsias and H. J. A. M. Heijmans, "Nonlinear multi-resolution signal decomposition schemes. Part I: Morphological pyramids," *IEEE Trans. Image Process.*, vol. 9, no. 11, pp. 1862–1876, Nov. 2000.
6. H. J. A. M. Heijmans and J. Goutsias, "Nonlinear multi-resolution signal decomposition schemes. Part II: Morphological wavelets," *IEEE Trans. Image Process.*, vol. 9, no. 11, pp. 1897–1913, Nov. 2000.
7. S. Li, B. Yang, and J. Hu, "Performance comparison of different multi resolution transforms for image fusion," *Inf. Fusion*, vol. 12, no. 2, pp. 74–84, 2011.
8. A. A. Goshtasby and S. Nikolov, "Image fusion: Advances in the state of the art," *Inf. Fusion*, vol. 8, no. 2, pp. 114–118, 2007.
9. R. Shen, I. Cheng, and A. Basu, "Cross-scale coefficient selection for volumetric medical image fusion," *IEEE Trans. Biomed. Eng.*, vol. 60, no. 4, pp. 1069–1079, Apr. 2013.
10. V. S. Petrovic and C. S. Xydeas, "Gradient-based multi-resolution image fusion," *IEEE Trans. Image Process.*, vol. 13, no. 2, pp. 228–237, Feb. 2004.
11. G.Pajares and J. M. de la Cruz, "A wavelet-based image fusion tutorial," *Pattern Recognit.*, vol. 37, no. 9, pp. 1855–1872, 2004.
12. G. Easley, D. Labate, and Wang-Q Lim, "Sparse directional image representations using the discrete shearlet transform," *Appl. Comput. Harmon. Anal.*, vol. 25, pp. 25–46, 2008.
13. K. A. Johnson and J. A. Becker. The whole brain atlas [Online]. Available: <http://www.med.harvard.edu/aanlib/>